JOURNAL OF MATERIALS SCIENCE 17 (1982) 369–376

# Fracture stress difference of notched polycarbonate between atmospheric pressure and a hydrostatic pressure

Y. KAIEDA
*Second Plastic Working Laboratory, Metal Processing Division, National Research Institute for Metals, 2-3-12 Nakameguro, Meguro-ku, Tokyo 153, Japan*

K. D. PAE
*High Pressure Materials Research Laboratory and Department of Mechanics and Materials Science, Rutgers University, New Brunswick, New Jersey 08903, USA*

Experimental data on fracture stress of polycarbonate (PC) with and without various artificial notches have been obtained at atmospheric pressure and a high hydrostatic pressure (400 MPa). The difference in fracture stress, $\Delta\sigma_F$, between both pressures was directly proportional to the intensity of pressure, $P$, and was inversely proportional to the stress concentration factor of the notch, $K_{\sigma n}$ such that $\Delta\sigma_F = 0.17\ P/K_{\sigma n}$ following the form of the Kaieda–Oguchi formula, $\Delta\sigma_F = P/K_\sigma$. By using the combined stress concentration factor, $K^*_{\sigma nc}$, of superposed notch and craze, and by considering the change in elastic modulus due to pressure, the experimental data agreed with the modified Kaieda–Oguchi formula. The stress concentration factor of the craze was calculated by using the Dugdale model.

## 1. Introduction

It has been shown, using maximum principal stress theory [1], that the fracture stress of brittle material increases with increasing pressure, i.e. $\sigma_{FP} - \sigma_{F0} = \Delta\sigma_F = P$, where $\sigma_{FP}$ and $\sigma_{F0}$ are fracture stresses under high pressure and at atmospheric pressure respectively, and $P$ is an absolute value of pressure. $\Delta\sigma_F$ is named the fracture stress difference. However, it was experimentally found that the brittle fracture stress under hydrostatic pressure was not always explained by the maximum principal stress theory if the sample was not coated appropriately [2]. This phenomenon has been explained by linear fracture mechanics as follows; the stress intensity factor, $K$, was not changed by pressure because the pressure transmitting medium penetrated to the surface flaw and balanced out the pressure acting on the surface of the specimen; therefore if the fracture toughness, $K_c$, under hydrostatic pressure is equal to that at atmospheric pressure, the fracture stress under hydrostatic pressure becomes equal to that at atmospheric pressure [2].

Recently Kaieda and Oguchi [3, 4] derived a simple formula relating the fracture stress difference due to hydrostatic pressure, $\Delta\sigma_F$, the intensity of pressure, $P$, and the stress concentration factor of the surface crack, $K_\sigma$, from the Griffith's fracture criterion. The formula is

$$\Delta\sigma_F = P/K_\sigma, \tag{1}$$

which agrees well with the experimental data for the intermetallic compound of the extremely brittle 100% $\sigma$-phase Fe–Cr alloy [3, 4] and $\gamma$-brass [5]. Moreover, when the blunting of the crack and the microplastic region at the root of the surface crack occurred, the formula was changed to

$$\Delta\sigma_F = P/K^*_\sigma, \tag{2}$$

where $K^*_\sigma$ is the plastic stress concentration factor of the blunted surface crack.

0022–2461/82/020369–08$2.80/0 

In polymers, Duckett [6] has also found the same formula as Kaieda and Oguchi. He found that the fracture stress of polymethylmethacrylate (PMMA) and polycarbonate (PC) increases linearly with increasing pressure. He explained the fracture stress increases in terms of the stress concentration of craze and the intensity of pressure.

PC, a glassy polymer, normally undergoes extensive deformation before fracture. However PC specimens of the geometry used for this study (a thick film) behaved like a very brittle material when they were tested in a silicone oil environment. No crazes were visible to the naked eye. It is well known that the stress–strain behaviour of the polymer is greatly affected by high hydrostatic pressure [7]. The relationship between the fracture stress, the intensity of pressure and the surface condition of polymers has not been studied in detail. In the present paper, the authors present experimental and theoretical studies of the factors influencing the fracture stress difference of PC with and without various artificial notches, at atmospheric pressure and at 400 MPa.

## 2. Theory

The detailed theory of brittle fracture stress under hydrostatic pressure is described elsewhere [3, 4], but a brief explanation is given here. A hydrostatic pressure is a uniform compressive force acting perpendicularly on the surface of a material, so that an isotropic material contracts elastically even though it may have a complicated shape. The stress distribution in the material under hydrostatic pressure is uniform and the stress, $\sigma$, equals $-P$ in any direction. When there is an internal crack in the material which is isolated from the pressure transmitting medium, the pressure acts to close the crack, as shown in Fig. 1a, because there is no force inside the crack to resist the pressure. If the crack has an elliptical shape of length $2c$, and tip radius $\rho$, there is a stress concentration at the tip of the internal crack. The maximum stress, $\sigma_{max}$, at the crack tip is

$$\sigma_{max} = -P(1 + 2\,[c/\rho]^{1/2}). \quad (3)$$

When there is a surface crack in the material which is penetrated by a pressure transmitting medium, as shown in Fig. 1b, the outer pressure acts as if to close the crack and the same intensive pressure inside the crack acts as if to open the crack and therefore cancels out the outer pressure. There is no stress concentration and a uniform stress distribution, which is equal to $-P$, is obtained everywhere in the material.

When there is a crack, having a stress concentration factor of $K_\sigma$, perpendicular to the tensile axis in the sample under high hydrostatic pressure, $-P$, and without applied load, the stress distribution ahead of the crack is seen to be different, depending on the type of crack, i.e., either an internal or a surface crack. In the case of the internal crack, the stress concentration occurs ahead of the crack tip. The maximum stress is $-K_\sigma P$ at the crack tip, and there is a uniform stress distribution of $\sigma = -P$ apart from the crack tip as shown in Fig. 2a. If, then, the material breaks from the internal crack, the applied stress required for fracture, $\sigma_{FP}$, equals $\sigma_{F0} + P$, where $\sigma_{F0}$ is the fracture stress at atmospheric pressure.

In the case of the surface crack, there is a uniform stress distribution of $\sigma = -P$, ahead of the crack under hydrostatic pressure as shown in Fig. 2b. The fracture occurs at atmospheric pressure in the stress distribution as shown in Fig.

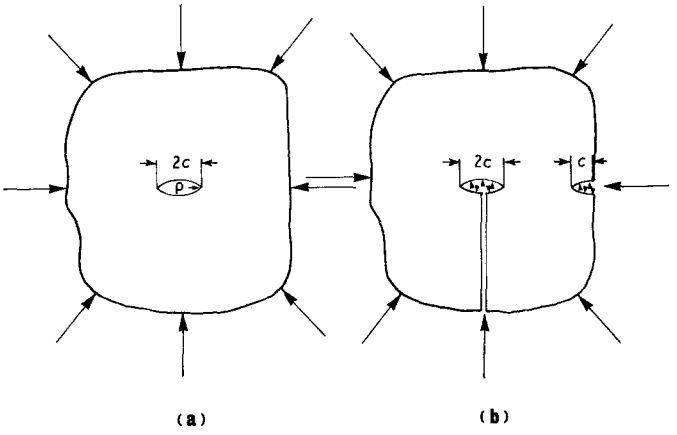


*Figure 1* Behaviour of materials which contain (a) an internal crack and (b) surface cracks to hydrostatic pressure.

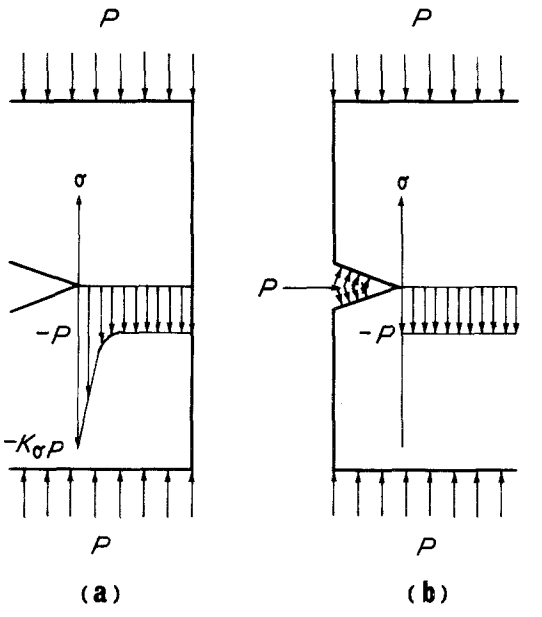


*Figure 2* Stress distribution in tensile specimens, without applied stress, under a hydrostatic pressure, with (a) an internal crack and (b) a surface crack.

3a and the applied stress is $\sigma_{F0}$. In the high hydrostatic pressure, the stress distribution at fracture is as shown in Fig. 3b, and the applied stress is $\sigma_{FP} = \sigma_{F0} + P/K_\sigma$.

If the surface crack is extremely sharp, then the fracture stress, $\sigma_{FP}$, under high hydrostatic pressure is the same as the fracture stress at atmospheric pressure, i.e. $\sigma_{FP} = \sigma_{F0}$. This is obtained from the Griffith energy balance theory [2, 3].

The fracture stress difference between a high hydrostatic pressure and atmospheric pressure is $\Delta\sigma_F = \sigma_{FP} - \sigma_{F0} = P/K_\sigma$ when the cause of fracture is the surface crack. $\Delta\sigma_F$ varies with $K_\sigma$ as shown in Fig. 4; the sharper the crack is, the smaller the fracture stress difference becomes. If there is an internal crack and a surface crack in the same sample, fracture occurs from the surface crack because the applied fracture stress due to the surface crack is smaller than that due to the internal crack.

## 3. Material and experimental procedure

The material used in the present experiment was obtained from a commercial source (Lexan polycarbonate, density = 1.2 g cm$^{-3}$). Samples were machined, taking care not to heat the samples during machining, to the form of the straight flat specimens with threaded ends for tensile testing as shown in Fig. 5. Various notch sizes were introduced at both sides of the central part of the specimens, as shown in Fig. 5.

The apparatus for tensile testing under hydrostatic pressure consisted of two interconnected thick-walled cylinders [7], one used for testing and the other used for pressure compensation. The applied force was measured by a full-bridge strain gauge which was mounted within the tensile testing shaft, unexposed to the pressure medium and unaffected by friction in the pressure seals. The elongation of the specimen was detected externally by a linear variable differential transformer. The tensile specimen was completely immersed in a hydrostatic pressure environment and the tensile stress was then superimposed. Testing speed was 0.02 mm sec$^{-1}$, therefore the test

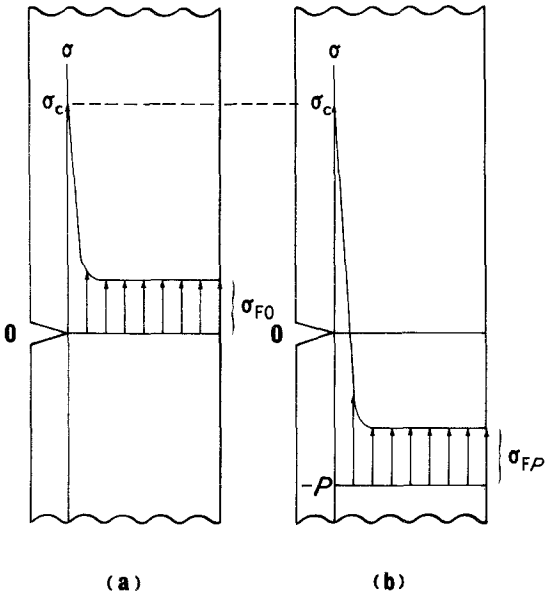


*Figure 3* Stress distribution ahead of a surface crack tip when fracture initiates from a surface crack at (a) atmospheric pressure and (b) at a high hydrostatic pressure $-P$.

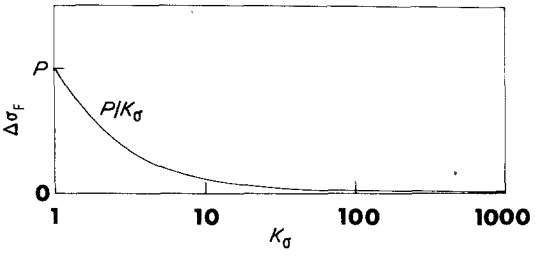


*Figure 4* The change in fracture stress difference, $\Delta\sigma_F$, due to pressure $P$ against the stress concentration factor of a surface crack.

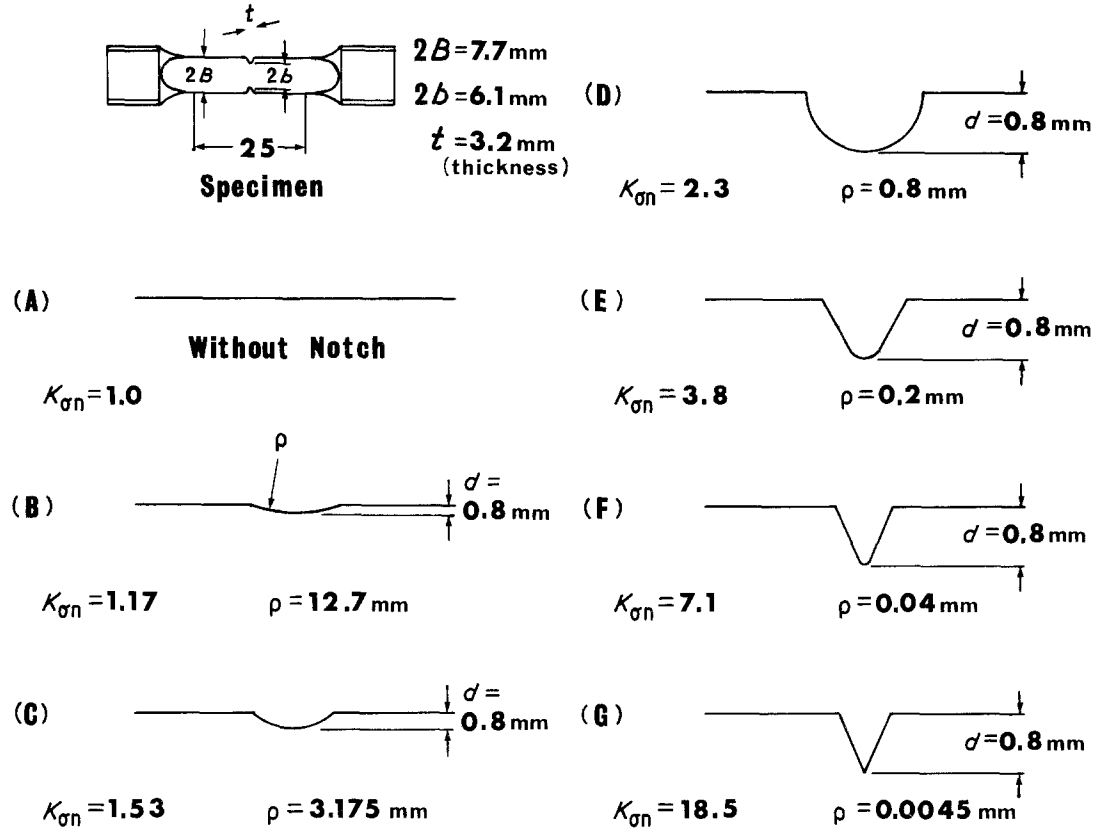


*Figure 5* A specimen, and the shape and stress concentration factor of the notches.

was assumed to be quasi-static. The pressure medium used in the present experiment was a silicone oil. At least five samples were tested for each kind of notched specimen at atmospheric pressure and at 400 MPa.

## 4. Notch shape and stress concentration factor

Notch shapes of the specimens are shown in Fig. 5. Type A has no notch and Type B to Type G have notches of 0.8 mm depth, with various notch-root radii. The stress concentration factor was calculated by the following experimental equation given by Heywood [8] from the results of the photoelastic experiment.

$$K_\sigma = 1 + \left( \frac{d/\rho}{1.55\, B/b - 1.3} \right)^n, \qquad (4)$$

where

$$n = \frac{(B/b - 1) + 0.5\,[d/\rho]^{1/2}}{(B/b - 1) + [d/\rho]^{1/2}}, \qquad (5)$$

and $B$, $b$, $d$ and $\rho$ represent geometric parameters as shown in Fig. 5. The calculated values of $K_\sigma$ from the above equations are also listed in Fig. 5.

## 5. Results and discussion

### 5.1. The relationship between fracture stress difference $\Delta\sigma_F$, intensity of pressure and stress concentration factor of notch

The tensile tests on the flat specimens (A) without a notch were carried out at pressures ranging from atmospheric pressure to 400 MPa at intervals of 100 MPa. The specimens were fractured at each pressure: the fractures were of brittle type and exhibited straight stress–strain curves and no ductility. The fracture stress increased linearly with increasing pressure. Then tensile tests on the specimens with various notches and without notch (A to G) were carried out at 0.1 MPa and at 400 MPa, at which pressures the minimum and maximum values of the fracture stresses were obtained. Every specimen underwent brittle fracture. The points marked in Fig. 6 are averaged values from at least five specimens tested at each pressure. There is some variation of the values (~ 15%)

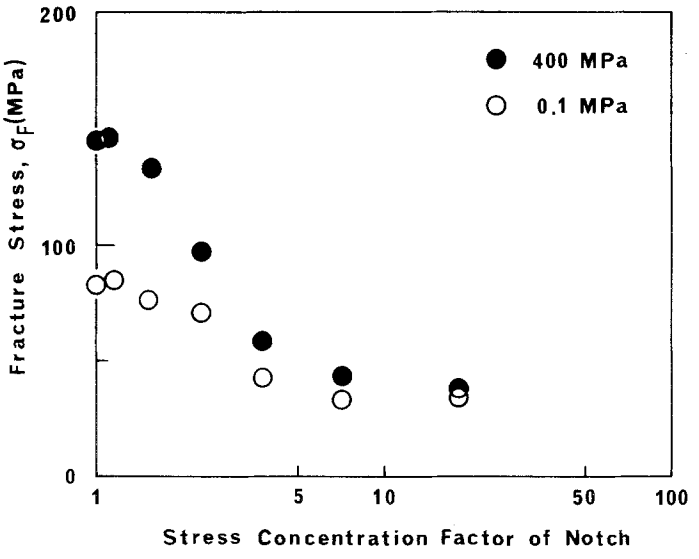


*Figure 6* Nominal brittle fracture stress at atmospheric pressure (open circles) and at 400 MPa (closed circles) against the stress concentration factor of the notch.

from specimen to specimen. It is obvious that the fracture stress decreases with increasing stress concentration factor and the fracture stress difference decreases also with the stress concentration factor. The samples of PC which fractured at both pressures are shown in Fig. 7.

The effect of the stress concentration factor of the notches on the difference in fracture stress between atmospheric pressure and 400 MPa is shown in Fig. 8. With increasing stress concentration factor of the notches, the fracture stress difference, $\Delta\sigma_F$, between atmospheric pressure and 400 MPa gradually decreases.

The data did not agree with the Kaieda–Oguchi formula [3, 4],

$$\Delta\sigma_F = P/K_{\sigma n} \quad (6)$$

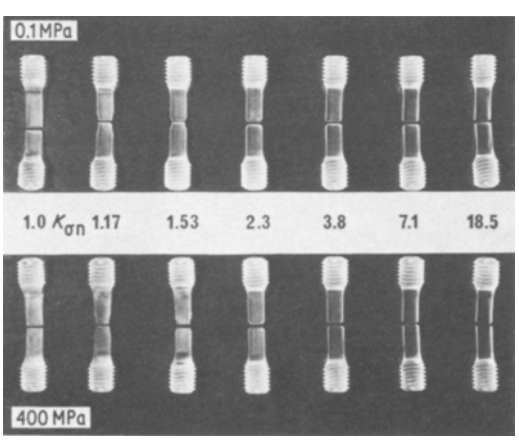


*Figure 7* Samples which fractured at atmospheric pressure and 400 MPa.

but the fact that fracture stress is inversely proportional to the stress concentration factor of the notch, $K_{\sigma n}$, agrees with the theory. A modified form of the Kaieda–Oguchi theory is proposed as,

$$\Delta\sigma_F = \alpha P/K_{\sigma n}, \quad (7)$$

where $\alpha$ is a constant. $\alpha$ was determined by the method of least squares to be 0.17. Thus Equation 7 becomes,

$$\Delta\sigma_F = 0.17\,P/K_{\sigma n}. \quad (8)$$

The reasons that $\alpha = 0.17$ for PC and $\alpha = 1$ for brittle metals are that the elastic modulus of PC changes with pressure but little or no change in elastic modulus is observed for metals, and also that stress crazing is involved in PC.

## 5.2. The effect of change in elastic modulus

One of the reasons that $\alpha = 0.17$ in Equation 7 rather than $\alpha = 1$ is the change in elastic modulus caused by applied pressure. The values of the Young's modulus of the present material at atmospheric pressure and at 400 MPa are shown in Table I. Even a brittle PC sample underwent yielding in the stress field where there was no tensile component but shear stress. The shear yield stress, $\tau_Y$, was 48 MPa at atmospheric pressure and 77 MPa at 400 MPa respectively. The values of tensile yield stress, $\sigma_Y$, estimated from the shear yield stress by the theory of Tresca at the same pressures as shown in Table I.

The critical stress, $\sigma_c$, of PC is considered to be increased at the same rate as the increase in elastic modulus due to pressure. Since the elastic

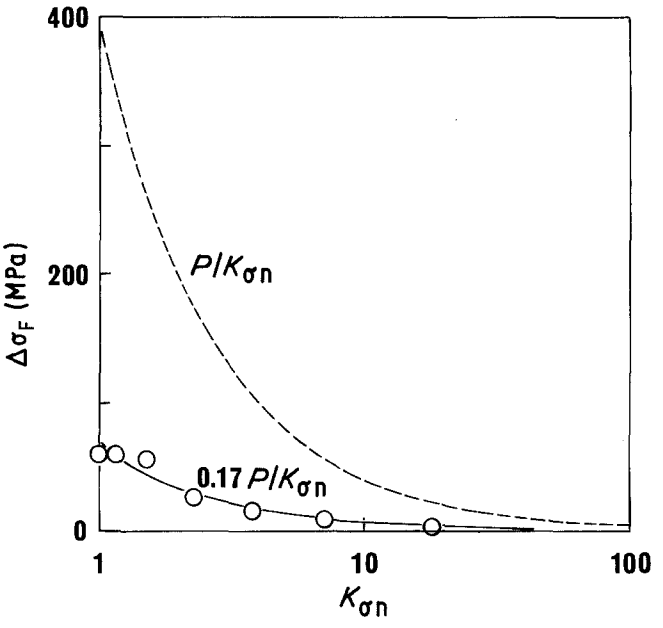


*Figure 8* Fracture stress difference, $\Delta\sigma_F$, between atmospheric pressure and 400 MPa against the stress concentration factor of the notch $K_{\sigma n}$.

modulus of PC is increased by pressure, the Equation 6 should be changed to,

$$\Delta\sigma_F = \frac{E_P}{E_0} \times \frac{P}{K_{\sigma n}}. \quad (9)$$

In the present experiment $E_P/E_0 = 1.57$ from Table I, therefore Equation 9 becomes

$$\Delta\sigma_F = 1.57\, P/K_{\sigma n}. \quad (10)$$

The effect of the change in elastic modulus due to hydrostatic pressure is incorporated in Equations 9 and 10. However, Equation 10 does not account for the experimental data, but points to the opposite direction.

## 5.3. The effect of the craze

It has been shown by Kitagawa and Kawagoe [9] and Mackay *et al.* [10], that PC crazes when subjected to stress and that craze is the origin of fractures. In the present experiment, a craze was initiated, in the material, at the root of the notch where the maximum stress exists, as shown in Fig. 9. The fracture may initiate at the tip of the craze. The craze grows to a maximum length just before fracture initiates.

TABLE I Values of Young's Modulus and estimated tensile Yield Stress of PC.

| Pressure (MPa) | $E$ (GPa) | $\sigma_Y$ (MPa) |
|---|---|---|
| 0.1 | 2.41 | 96 |
| 400 | 3.79 | 154 |

The shape of the craze was clarified by Argon and Salama [11] as shown in Fig. 10. The craze has a very thin highly oriented porous structure and the fraction of craze matter tufts in the craze is small. Therefore the stress concentration factor of the craze can be expressed as follows,

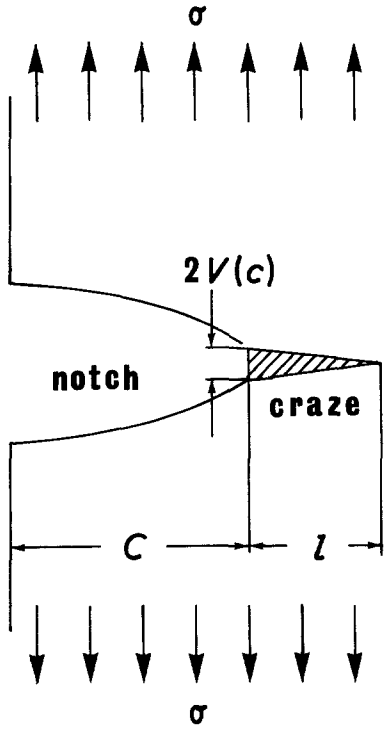


*Figure 9* Schematic drawing of an artificial notch and craze.

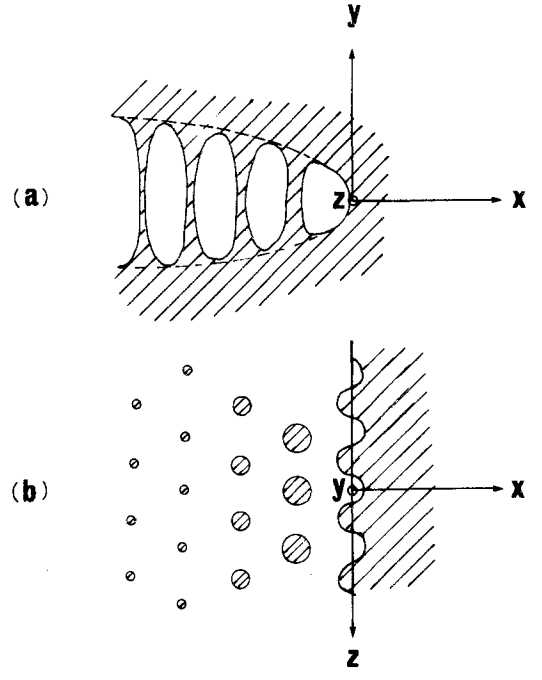


*Figure 10* Schematic drawing of a craze, showing (a) the outline of craze tip, and (b) the cross-section in the craze-plane across the craze matter tufts. (After Argon and Salama, 1977, courtesy of Taylor and Francis Ltd.)

$$K^*_{\sigma c} = 1 + 2[l/\rho]^{1/2}, \qquad (11)$$

where $l$ is the craze length and $\rho$ is the tip radius which is approximaterly equal to the half of the craze thickness. Moreover, the effect of the craze may be considered as a combination of the craze and the notch as shown in Fig. 9.

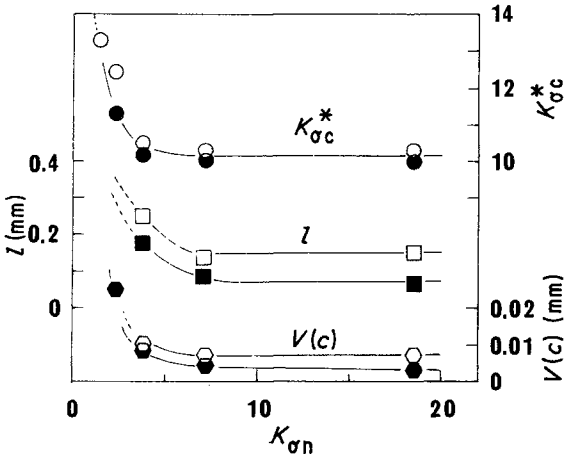


*Figure 11* Length $l$, opening displacement $V(c)$ and stress concentration factor $K^*_{\sigma c}$ of the craze against stress concentration factor, $K_{\sigma n}$ of a notch at atmospheric pressure (open symbols) and 400 MPa (closed symbols).

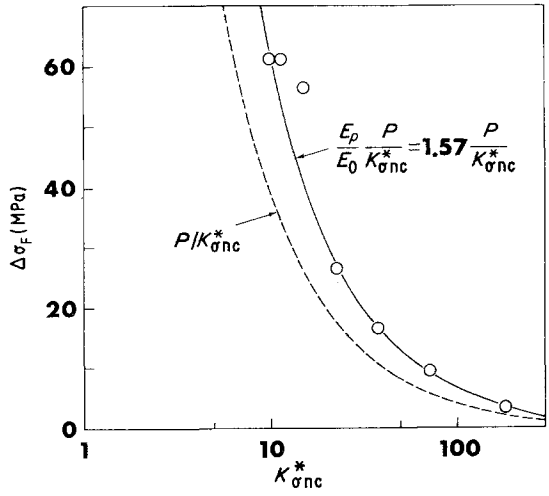


*Figure 12* Fracture stress difference, $\Delta\sigma_F$, against superposed stress concentration factor, $K^*_{\sigma nc}$, of notch and craze.

## 5.4. Calculation of the stress concentration factor of the craze from the Dugdale model

Graham *et al.* [12] indicated that the relationship between the applied stress and the craze length was explained by the Dugdale model [13] which determined the plastic zone size at the root of the notch under tensile stress in a non-strain-hardening material. The present authors applied the Dugdale model to their experiment and calculated the stress concentration factor of the craze. The relationship [13] between the craze length, $l$, the notch length, $c$, the applied stress, $\sigma$, and the yield stress, $\sigma_Y$, is,

$$\frac{c}{c+l} = \cos\left(\frac{\pi}{2}\frac{\sigma}{\sigma_Y}\right), \qquad (12)$$

where

$$l = c\left[\sec\left(\frac{\pi}{2}\frac{\sigma}{\sigma_Y}\right) - 1\right]. \qquad (13)$$

The craze opening displacement, $2V(c)$, is related to the craze length [14] by

$$V(c) = \frac{4\sigma_Y c}{\pi E}\ln\left(\frac{l+c}{c}\right), \qquad (14)$$

and is a function of the applied stress, $\sigma$, as

$$V(c) = \frac{4\sigma_Y c}{\pi E}\ln\left[\sec\left(\frac{\pi}{2}\frac{\sigma}{\sigma_Y}\right)\right]. \qquad (15)$$

From Equation 11 the stress concentration factor of the craze becomes

$$K^*_{\sigma c} = 1 + 2[l/V(c)]^{1/2}, \quad (16)$$

$$= 1 + \left\{ \pi E \left[ \sec\left( \frac{\pi}{2} \frac{\sigma}{\sigma_Y} \right) - 1 \right] \Big/ \sigma_Y \ln\left[ \sec\left( \frac{\pi}{2} \frac{\sigma}{\sigma_Y} \right) \right] \right\}^{1/2} \quad (17)$$

The maximum length of the craze is obtained when $\sigma = \sigma_F$ at both pressures. The values of $l$, $V(c)$ and $K_\sigma$ at both pressures, calculated by using the values of Table I and the fracture stress at both pressures, are shown in Fig. 11. The stress concentration factor of the craze is almost constant in the range of the factor of the notch $K_{\sigma n} \cong 5$ to 20, and $l$, $V(c)$ and $K^*_{\sigma c}$ increase steeply in the range of $K^*_{\sigma c} \leqslant 5$.

However, Bessonov and Kuvshinsky [15] have revealed that the craze thickness increases with craze length, therefore the stress concentration factor of the craze is assumed to be almost constant. Then, the values of $l$, $V(c)$ and $K^*_{\sigma c}$ in the range of small $K_{\sigma n}$ do not increase significantly, but this means the Dugdale model agrees well with experimental data in the case of sharper notch. A stress concentration factor of the craze, $K^*_{\sigma c} = 10$, is used in this paper.

### 5.5. The effect of the stress concentration factor of the superposed notch and craze

When there is a small notch at the root of a large notch, the stress concentration factor of the superposed notch is in general the product of the factor of each notch [16]. Then the superposed stress concentration factor, $K^*_{\sigma nc}$ of the notch and craze is expressed as

$$K^*_{\sigma nc} \cong K_{\sigma n} \times K^*_{\sigma c}. \quad (18)$$

The experimental values of the fracture stress difference between 0.1 and 400 MPa with superposed stress concentration factor, $K^*_{\sigma nc}$, are shown in Fig. 12, and the modified Equations 6 and 10, in which $K_{\sigma n}$ is replaced by $K^*_{\sigma nc}$, are also drawn together in Fig. 12. In Fig. 12 the values of the fracture difference against $K^*_{\sigma nc}$ agree quite well with the curve of the Equation 10, i.e. $1.57P/K^*_{\sigma nc}$. This result shows that the increase in fracture stress of the notched PC under hydrostatic pressure is described by the intensity of pressure and the superposed stress concentration factor of the notch and craze and the ratio of the elastic modulus at pressure $E_P$ to the elastic modulus at atmospheric pressure, $E_0$. This relation is expressed as

$$\sigma_{FP} - \sigma_{F0} = \Delta\sigma_F = \frac{E_P}{E_0} \frac{P}{K^*_{\sigma nc}}. \quad (19)$$

## 6. Conclusion

Fracture stress of polycarbonate with and without various artificial notches increased under high hydrostatic pressure. The fracture stress increase $\Delta\sigma_F$ was influenced by the intensity of pressure $P$, the ratio of the elastic constant changed by pressure $E_P/E_0$, and the stress concentration factor of the superposed notch and craze $K^*_{\sigma nc}$; and was expressed as

$$\Delta\sigma_F = \frac{E_P}{E_0} \frac{P}{K^*_{\sigma nc}}.$$


## Acknowledgement

The authors wish to thank Dr. A. Oguchi of the National Research Institute for Metals, Tokyo, and Prof. N. Inoue of the Science University of Tokyo for their helpful discussion.


## References


1. H. Ll. D. PUGH, "Mechanical Behaviour of Materials under Pressure" (Elsevier Publishing Co., Amsterdam New York and Oxford, 1970) p. 277.
2. M. SAKATA and S. AOKI, *J. Soc. Mat. Sci. Japan* **22** (1973) 532.
3. Y. KAIEDA and A. OGUCHI, *J. Japan Inst. Metals* **43** (1979) 161.
4. *Idem, Trans. Japan Inst. Metals* **22** (1981) 83.
5. *Idem, ibid.* **22** (1981) 326.
6. R. A. DUCKETT, *J. Mater. Sci.* **15** (1980) 2471.
7. J. A. SAUER, D. R. MEARS and K. D. PAE, *European Polymer J.* **6** (1970) 1015.
8. R. B. HEYWOOD, "Designing by Photoelasticity" (Chapman and Hall, London, 1952) p. 163.
9. M. KITAGAWA and M. KAWAGOE, *J. Mater. Sci.* **14** (1979) 953.
10. M. E. MACKAY, T. G. TENG and J. M. SCHULTZ, *J. Mater. Sci.* **14** (1979) 221.
11. A. S. ARGON and M. M. SALAMA, *Phil. Mag.* **36** (1977) 1217.
12. I. D. GRAHAM, J. G. WILLIAMS and E. L. ZICHY, *Polymer* **17** (1976) 439.
13. D. S. DUGDALE, *J. Mech. Phys. Solids* **8** (1960) 100.
14. G. T. HAHN and A. R. ROSENFIELD, *Acta. Metall.* **13** (1965) 293.
15. M. I. BESSONOV and E. V. KUVSHINSKY, *Sov. Phys. Solid State* **3** (1961) 950.
16. V. VINCENTINI, *Exp. Mech.* **7** (1967) 117.



*Received 27 February*
*and accepted 1 July 1981*